

A new spectroscopic calibration to determine T_{eff} and [Fe/H] of FGK dwarfs and giants

G. D. C. Teixeira^{1,2,*}, S. G. Sousa¹, M. Tsantaki^{1,3}, M. J. P. F. G. Monteiro^{1,2}, N. C. Santos^{1,2}, and G. Israelian^{4,5}

¹*Instituto de Astrofísica e Ciências do Espaço, Universidade do Porto, CAUP, Rua das Estrelas, 4150-762 Porto, Portugal*

²*Departamento de Física e Astronomia, Faculdade de Ciências, Universidade do Porto, Rua do Campo Alegre, 4169-007 Porto, Portugal*

³*Instituto de Radioastronomía y Astrofísica, IRyA, UNAM, Campus Morelia, A.P. 3-72, C.P. J8089 Michoacán, Mexico*

⁴*Instituto de Astrofísica de Canarias, 38200 La Laguna, Tenerife, Spain*

⁵*Departamento de Astrofísica, Universidad de La Laguna, 38206 La Laguna, Tenerife, Spain*

Abstract. We present a new spectroscopic calibration for a fast estimate of T_{eff} and [Fe/H] for FGK dwarfs and GK giant stars. We used spectra from a joint sample of 708 stars, composed by 451 FGK dwarfs and 257 GK-giant stars with homogeneously determined spectroscopic stellar parameters. We have derived 322 EW line-ratios and 100 FeI lines that can be used to compute T_{eff} and [Fe/H], respectively. We show that these calibrations are effective for FGK dwarfs and GK-giant stars in the following ranges: $4500\text{ K} < T_{\text{eff}} < 6500\text{ K}$, $2.5 < \log g < 4.9\text{ dex}$, and $-0.8 < [\text{Fe}/\text{H}] < 0.5\text{ dex}$. The new calibration has a standard deviation of 74 K for T_{eff} and 0.07 dex for [Fe/H]. We use four independent samples of stars to test and verify the new calibration, a sample of giant stars, a sample composed of Gaia FGK benchmark stars, a sample of GK-giant stars from the DR1 of the Gaia-ESO survey, and a sample of FGK-dwarf stars. We present a new computer code, GeTCal, for automatically producing new calibration files based on any new sample of stars.

1 Introduction

Deriving accurate and precise stellar parameters is a fundamental aspect of astrophysical studies. In order to determine the mass, radius, and age of stars it is necessary to measure stellar atmospheric parameters, such as effective temperature (T_{eff}), surface gravity ($\log g$), metallicity ([Fe/H]), and microturbulence (v_{mic}), obtained mainly by spectroscopic or photometric methods (e.g. Casagrande et al. [3], Sousa et al. [12], Tsantaki et al. [20]).

The volume of data being produced by large-survey observational programs [2, 4] requires the existence of quick methods to obtain stellar parameters for a diverse range of stellar spectral types.

Methods such as line-strength ratios can be used to obtain T_{eff} [5, 6, 9], and equivalent widths (EWs) of FeI can be used to derive [Fe/H] [15]. The success of these methods is tied to the quality of the empirical calibrations.

One of the spectroscopic methods that can be used to determine spectral parameters is the ARES+MOOG method. This method makes use of the ARES code (to measure the EWs of a spectrum [11, 17]), and the MOOG code (to measure individual line abundances) combined with a minimization algorithm in order to derive the parameters of the stellar atmosphere [18]. For a more detailed description of this method see Sousa [16].

An automated tool, TMCALC, can be used to obtain T_{eff} and [Fe/H] using measurements of EWs of spectral lines [15]. It relies on EW line-ratios and on the EWs of FeI lines. The accuracy and precision of this TMCALC are mainly limited by the T_{eff} and [Fe/H] calibrations [15]. TMCALC is less accurate than the ARES+MOOG method but it is computationally more efficient.

The main body of this work was presented in detail in Teixeira et al. [19].

2 Stellar samples

We used six distinct stellar samples: two samples were used for calibration and four other samples were used for independent testing of the new calibration. A summary of each sample can be found in Table 1.

The parameters for each sample have been consistently determined homogeneously with ARES+MOOG. The samples used were:

- 451 FGK-dwarf stars described in Sousa et al. [12] that was revised in Tsantaki et al. [20], hereafter the So08 sample.
- 257 giant stars from Alves et al. [1], hereafter the A115 sample.
- 44 giant stars from Santos et al. [10], hereafter the Sa09 sample.

*e-mail: guilherme.teixeira@astro.up.pt

Table 1: Summary of the stellar samples.

Sample	stars	stars_used	(S/N)	Spec type	T_{eff} (K)	$\log g$ (dex)	v_{mic} (kms^{-1})	[Fe/H] (dex)
So08	451	451	[70, 2000]	FGK	[4400, 6431]	[3.60, 4.82]	[0, 2.1]	[-0.83, 0.36]
A115	257	257	~ 150	GK	[4724, 5766]	[2.37, 3.92]	[1.08, 4.28]	[-0.75, 0.27]
Sa09	56	44	~ 200	GK	[4157, 6020]	[1.15, 4.82]	[0.86, 2.26]	[0, 0.32]
Gaia	34	18	[200, 400]	FGK	[3472, 6635]	[0.51, 4.67]	[0.89, 1.92]	[-2.64, 0.35]
GES	36	36	~ 100	GK	[4753, 5289]	[2.50, 3.86]	[1.17, 4.06]	[-0.51, 0.25]
So11	582	582	[100, 200]	FGK	[4487, 7212]	[3.61, 4.96]	[0, 2.87]	[-1.14, 0.55]

Table 2: Limits of applicability of the Te16 calibration.

T_{eff} (K)	$\log g$ (dex)	[Fe/H] (dex)
[4500, 6500]	[2.5, 4.9]	[-0.8, 0.5]

- 18 benchmark stars of the Gaia survey, hereafter the Gaia sample [7, 8].
- 36 GK-giant stars from the Gaia-ESO survey DR1¹ with $\log g < 3.9$, hereafter the GES sample.
- 582 FGK-dwarf stars from Sousa et al. [14] with well-determined parameters, hereafter the So11 sample.

For calibration, we used a combination of the So08 and A115 samples, hereafter the joint sample. The other sample were used to test our new calibration.

3 Calibration

This work aimed to build new T_{eff} and [Fe/H] spectroscopic calibrations for both FGK dwarfs and GK giants improving upon the work of Sousa et al. [15], hereafter the So12 calibration. The rationale for each step of the calibration procedure can be found in Teixeira et al. [19].

3.1 T_{eff} calibration

In order to obtain the T_{eff} calibration we used the established relations between EW line-ratios, R_{EW} [13]. This technique is based on the different sensitivity that metal lines have to T_{eff} . EW line-ratios are more precise than the use of EWs of individual lines [5, 6, 9, 13].

To compute the T_{eff} calibration we:

- Selected lines with a difference in excitation potential greater than 3 eV.
- Selected only lines in close proximity, ($\Delta\lambda < 70\text{\AA}$).
- Discarded ratios when $R_{\text{EW}} \notin [0.01, 100]$.
- Fitted a linear and a third-degree polynomial function to the distributions of T_{eff} as a function of: a) R_{EW} ; b) $1/R_{\text{EW}}$; and c) $\log R_{\text{EW}}$.

¹https://www.gaia-eso.eu/sites/default/files/file_attach/ESO-DR1-release-description.pdf

- Performed a cut-off based on the interquartile range method, IQR [21].
- Used a $2\text{-}\sigma$ cut on the distributions, refitted the functions and selected the fit with the smaller standard deviation.
- Only accepted a function that could fit 2/3 of the calibration sample.

3.2 Metallicity calibration

We calibrated the metallicity using only iron absorption lines, as iron abundance is a proxy for stellar metallicity [15]. We discarded ionized iron lines given their dependence on $\log g$.

We obtained the metallicity calibration by:

- Considering only lines with $\text{EW} < 70 \text{ m\AA}$.
- Excluded lines with $\text{EW} < 20 \text{ m\AA}$.
- Solved equation:

$$\begin{aligned} \text{EW} = & C_0 + C_1 \times [\text{Fe}/\text{H}] + C_2 \times T_{\text{eff}} + \\ & C_3 \times [\text{Fe}/\text{H}]^2 + C_4 \times T_{\text{eff}}^2 + \\ & C_5 \times [\text{Fe}/\text{H}] \times T_{\text{eff}} . \end{aligned} \quad (1)$$

- Applied the IQR and a $2\text{-}\sigma$ to a linear fit made with the inversion of the previous equation.
- Made sure that the slope of the comparison between the calibrated and spectroscopic [Fe/H] was within 3% of the identity line.
- Only considered lines if the function had $\sigma < 0.06 \text{ dex}$.

3.3 GeTCal

As a by-product of our work we created a Python code: GeTCal. This code is a practical implementation of the methods described in Sects. 3.1 and 3.2 and is able to automatically produce T_{eff} and [Fe/H] calibrations. As input it requires three parameters: a line list, the stellar parameters (and errors) of a sample of stars, and the measured EWs for each star. The calibrations produced by GeTCal can then be used to compute the T_{eff} and [Fe/H] for stars of spectral classes similar to the calibration sample. The code can perform the T_{eff} calibration, the [Fe/H] calibration, or both simultaneously.

GeTCal is built in such a way as to produce output calibration files which are compatible with the TMCALC

Table 3: Application of the Te16 calibration to the samples.

Sample	ΔT_{eff} (K)	$\Delta T_{\text{eff_median}}$ (K)	$\Delta T_{\text{eff_}\sigma}$ (K)	$\Delta[\text{Fe}/\text{H}]$ (dex)	$\Delta[\text{Fe}/\text{H}]_{\text{median}}$ (dex)	$\Delta[\text{Fe}/\text{H}]_{\sigma}$ (dex)
So08	17	23	76	0.01	0.02	0.04
A115	-32	-36	58	-0.07	-0.06	0.08
Joint	-1	-8	74	-0.02	0.00	0.07
GES	20	38	141	0.05	0.06	0.11
Sa09	-44	-41	75	-0.04	-0.06	0.10
Gaia	43	40	91	0.08	0.09	0.18
So11	47	46	89	0.02	0.02	0.05
Combined-validation	40	37	93	0.02	0.02	0.07

code [15]. This code is freely distributed and available for use by the community ².

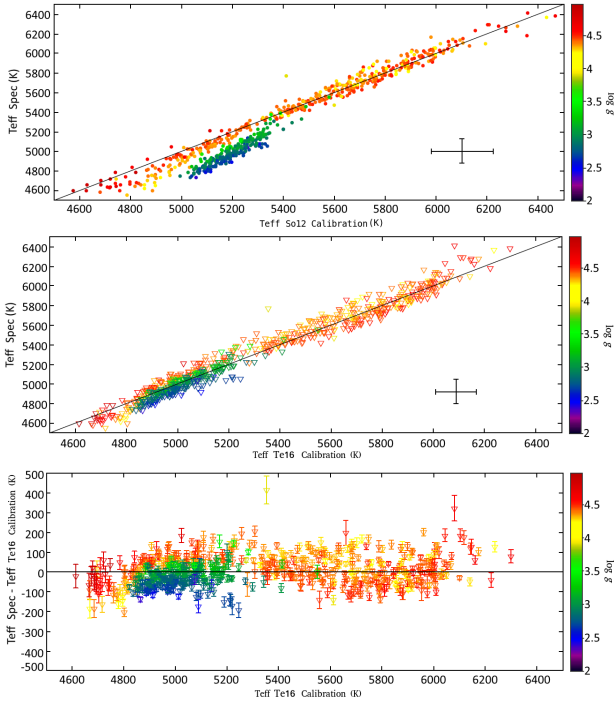


Figure 1: Comparison between the T_{eff} computed in this work and the spectroscopic values with the So12 calibration (top panel) and the Te16 calibration (middle panel) for the joint sample. The line in the two plots represents the identity line, the standard deviation is plotted as the cross in both panels. In the bottom panel we show the difference between the Te16 calibration and the spectroscopic T_{eff} as a function of T_{eff} , the error bars represent the errors in our computation. The plots are colour-coded for $\log g$. Figure from [19].

4 Results

Figure 1 compares the computed T_{eff} with the spectroscopic T_{eff} using the different calibrations. The top panel of Fig. 1 shows the previous calibration, the middle panel shows the new calibration and the bottom panel shows the

²The GeTCaI code and the T_{eff} and $[\text{Fe}/\text{H}]$ calibrations are available at <http://www.astro.up.pt/exoearths/tools.html>.

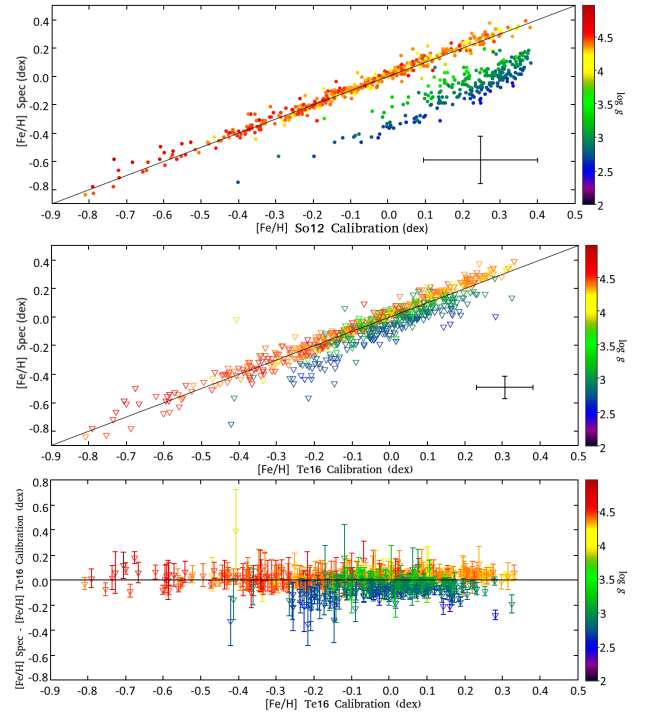


Figure 2: Comparison between the $[\text{Fe}/\text{H}]$ computed in this work and the spectroscopic values for the So12 calibration (top panel) and the Te16 calibration (middle panel) for the joint sample. The black line represents the identity line, the standard deviation is shown as the cross. The bottom panel shows the difference between $[\text{Fe}/\text{H}]$ from spectroscopy and the one in this work as a function of $[\text{Fe}/\text{H}]$, the error bars are the errors resulting from this work. The plots are colour-coded for $\log g$. Figure from [19].

difference between the new calibration and the spectroscopic values. The Te16 calibration improves in the low T_{eff} and low $\log g$ regimes, i.e., the giants.

Figure 2 shows the same type of analysis but now for the computed $[\text{Fe}/\text{H}]$. The bottom panel shows most stars well within 0.2 dex from the zero value.

As shown in Table 3, for the joint sample, the T_{eff} standard deviation is 74 K, and the standard deviation of $[\text{Fe}/\text{H}]$ is 0.07 dex for the Te16 calibrations.

The limits of the Te16 calibration reflect the parameters of the calibration sample and are presented in Table 2.

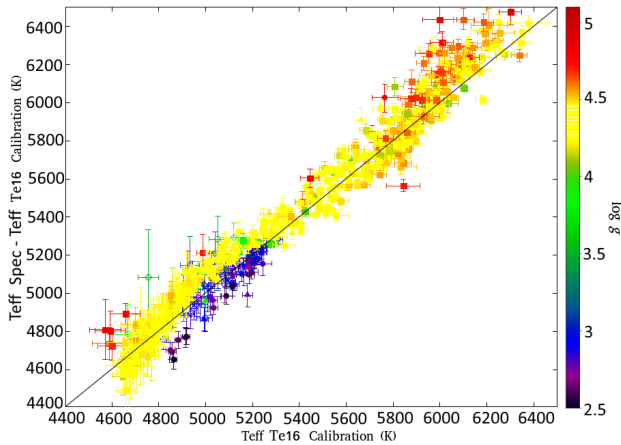


Figure 3: Comparison between the T_{eff} computed with TMCALC and the spectroscopic values with the Te16 calibration for the Gaia (closed triangles), Sa09 (circles), GES (open diamonds), and So11 (closed squares) sample. The colour-code represents the $\log g$ values and the black line represents the identity line. Only stars within the limits of applicability are plotted.

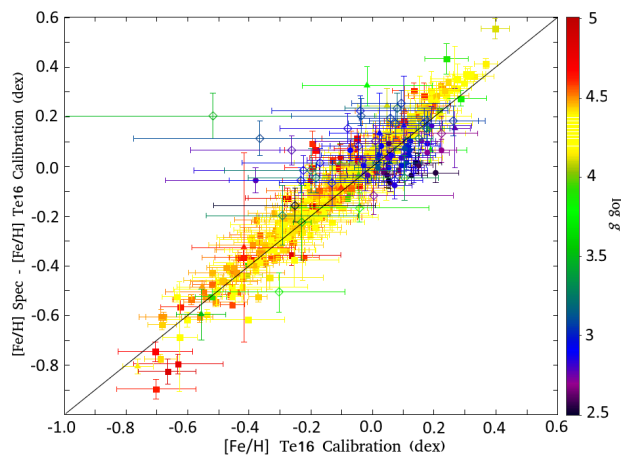


Figure 4: Comparison between the $[\text{Fe}/\text{H}]$ computed with TMCALC and the spectroscopic values with the Te16 calibration for Gaia (closed triangles), Sa09 (circles), GES (open diamonds), and So11 (closed squares) sample. The colour-code represents the $\log g$ values and the black line represents the identity line. Only stars within the limits of applicability are plotted.

Higher uncertainties will result from using the Te16 calibration outside the applicability limits [19].

After obtaining the Te16 calibration for T_{eff} and $[\text{Fe}/\text{H}]$, we applied it to the four independent samples. Figure 3 shows the comparison of T_{eff} results between the Te16 calibration and the values from spectroscopy for the validation samples. Stars outside the limits of the Te16 calibration ($\log g < 2.5$) are not plotted.

The results for the $[\text{Fe}/\text{H}]$ computation of the independent samples are shown in Fig. 4. The outliers are stars with low- $\log g$ values and T_{eff} and, therefore, very close to our applicability limits (see Table 2).

A summary of the application of the Te16 calibration to the various validation samples is provided in Table 3.

5 Conclusions

We presented new calibrations to obtain T_{eff} and $[\text{Fe}/\text{H}]$ from the EWs of stellar spectra. These calibrations cover both FGK dwarfs and GK giants simultaneously [19]. The Te16 calibration is effective within the range of $4500\text{K} < T_{\text{eff}} < 6500\text{K}$, $2.5 < \log g < 4.9$ dex, and $-0.8 < [\text{Fe}/\text{H}] < 0.5$ dex.

We built a Python code, GeTCAL, capable of computing T_{eff} and $[\text{Fe}/\text{H}]$ calibrations for any given sample of calibration stars. This program produces calibration files compatible with the existing TMCALC code.

This work provides a fast way to determine stellar atmospheric parameters from spectrographic observations of FGK-dwarf and GK-giant stars.

Acknowledgments

G.D.C.T. was supported by a research fellowship (CAUP2013-05UnI-BI), funded by the European Commission through project SPACEINN (FP7-SPACE-2012-312844) and by an FCT/Portugal PhD grant PD/BD/113478/2015. Part of this work was supported by FCT/Portugal (UID/FIS/04434/2013) and COMPETE2020 (POCI-01-0145-FEDER-007672).

References

- [1] Alves, S., Benamati, L., Santos, N. C., et al. *MNRAS*, **448**, 2749 (2015)
- [2] Bland-Hawthorn, J., Sharma, S., & Freeman, K. *EAS Publications Series*, **67**, 219 (2014)
- [3] Casagrande, L., Ramírez, I., Meléndez, J., Bessell, M., Asplund, M., *A&A*, **512**, A54 (2010)
- [4] Gilmore, G., Randich, S., Asplund, M., et al., *The Messenger*, **147**, 25 (2012)
- [5] Gray, D. F. *Stellar Surface Structure*, **176**, 227 (1996)
- [6] Gray, D. F., *The Observation and Analysis of Stellar Photospheres*, 3rd Edition (ISBN 0521851866. , UK: Cambridge University Press, 2005)
- [7] Heiter, U., Jofré, P., Gustafsson, B., et al., *A&A*, **582**, A49 (2015)
- [8] Jofré, P., Heiter, U., Soubiran, C., Blanco-Cuaresma, S. et al., *A&A*, **564**, A133 (2014)
- [9] Kovtyukh, V. V., Soubiran, C., Belik, S. I., Gorlova, N. I., *A&A*, **411**, 559 (2003)
- [10] Santos, N. C., Lovis, C., Pace, G., Melendez, J., Naef, D., *A&A*, **493**, 309 (2009)
- [11] Sousa, S. G., Santos, N. C., Israelian, G., Mayor, M., & Monteiro, M. J. P. F. G., *A&A*, **469**, 783 (2007)
- [12] Sousa, S. G., Santos, N. C., Mayor, M., et al., *A&A*, **487**, 373 (2008)
- [13] Sousa, S. G., Alapini, A., Israelian, G., & Santos, N. C., *A&A*, **512**, A13 (2010)
- [14] Sousa, S. G., Santos, N. C., Israelian, G., Mayor, M., & Udry, S. *A&A*, **533**, A141 (2011)
- [15] Sousa, S. G., Santos, N. C., & Israelian, G., *A&A*, **544**, A122 (2012)

- [16] Sousa, S., arXiv:1407.5817 (2014)
- [17] Sousa, S. G., Santos, N. C., Adibekyan, V., Delgado-Mena, E., & Israelian, G., *A&A*, **577**, A67 (2015)
- [18] Sneden, C. A. Ph.D. Thesis, The University of Texas at Austin (1973)
- [19] Teixeira, G. D. C., Sousa, S. G., Tsantaki, M., et al. 2016, *A&A*, **595**, A15
- [20] Tsantaki, M., Sousa, S. G., Adibekyan, V. Z., et al., *A&A*, **555**, A150 (2013)
- [21] Upton, G., Cook, I., *Understanding Statistics* (Oxford University Press., 1996)